

A STUDY OF THERMAL RESPONSE
OF THE LUNAR SURFACE AT THE LANDING SITE
DURING THE DESCENT OF THE LUNAR EXCURSION MODULE (LEM)

by

Jerome T. Holland and Hector C. Ingrao

Harvard College Observatory
Cambridge, Massachusetts (USA)

Technical Report

April 1, 1966

Prepared For
ARTHUR D. LITTLE, INC.
Cambridge, Mass.

and
NATIONAL AERONAUTICS AND SPACE ADMINISTRATION
NASA RESEARCH GRANT NO. Nsg 64-60

NOTE

We are indebted to Mr. Alfred Wechsler of Arthur D. Little who supplied the boundary conditions of the heat transfer problem given in Sections III and IV.

A STUDY OF THERMAL RESPONSE OF THE
LUNAR SURFACE AT THE LANDING SITE DURING
THE DESCENT OF THE LUNAR EXCURSION MODULE (LEM)

Jerome T. Holland* and Hector C. Ingrao**

ABSTRACT

32298

This report analyzes the thermal response of the lunar surface at the landing site due to the radiative and convective heat transfer from the LEM exhaust nozzle. A computer program has been written to analyze the thermal transients as a function of 1) the thermal model of the lunar surface materials; 2) depth beneath the lunar surface; 3) distance from the touchdown point. The physical meaning of the answers obtained in our analysis depends on how accurate the heat transfer parameters are for the assumed model, during the LEM descent. Therefore we prefer to stress the method of analysis rather than the numerical conclusions.

* Senior Analyst, Harvard Computing Center

** Senior Research Associate and Project Director, Harvard College
Observatory

CONTENTS

<u>I.</u>	<u>INTRODUCTION</u>	1
<u>II.</u>	<u>SCIENTIFIC OBJECTIVE</u>	2
<u>III.</u>	<u>HEAT TRANSFER ON THE LUNAR SURFACE</u>	4
	A. Irradiance on the Surface Produced by LEM	4
	B. Radiant Emittance From Lunar Surface to Space	6
	C. Irradiance on the Surface by the Sun	6
<u>IV.</u>	<u>ASSUMED THERMAL PARAMETERS FOR THE LUNAR SURFACE</u>	9
<u>V.</u>	<u>LANDING SITE AND TIME</u>	10
<u>VI.</u>	<u>HEAT FLOW EQUATIONS</u>	11
<u>VII.</u>	<u>THERMAL MODELS OF THE LUNAR SURFACE</u>	14
<u>VIII.</u>	<u>INITIAL CONDITIONS</u>	15
<u>IX.</u>	<u>BOUNDARY CONDITIONS</u>	18
<u>X.</u>	<u>COMPUTER OUTPUT</u>	20
	<u>APPENDICES</u>	29
	<u>REFERENCES</u>	46

NOTATIONS AND UNITS

- C = equivalent capacitance, F
 c = specific heat of lunar material, $J\ gm^{-1}\cdot K^{-1}$
 d = distance from LEM point of touchdown, ft
 F_{ns} = view factor from differential surface element to rocket nozzle
 F_{ss} = view factor from differential surface element to LEM exhaust shield
 $g_c(H,d)$ = convection heat transfer coefficient from LEM, $W\ cm^{-2}\cdot C^{-1}$
 $g_c(t)$ = gas heat transfer coefficient, d constant, $W\ cm^{-2}\cdot C^{-1}$
 $g_c(d)$ = gas heat transfer coefficient, t constant, $W\ cm^{-2}\cdot C^{-1}$
 H = elevation of LEM above surface, ft
 H_n = height of LEM nozzle above surface, ft
 H_s = height of the heat shield above the surface, ft
 I = equivalent current, A
 J = irradiance by the sun on lunar surface, $W\ cm^{-2}$
 J_0 = irradiance by the sun on lunar surface at $z = 0$, $W\ cm^{-2}$
 $P(x)$ = approximate phase angle of thermal wave at depth, x
 Q_{LEM} = irradiance by the LEM on the lunar surface, $W\ cm^{-2}$
 Q_{rs} = radiant emittance from the lunar surface, $W\ cm^{-2}$
 $Q(x,t)$ = flux density at depth, x , and time, t , $W\ cm^{-2}$
 R = equivalent resistance, Ω
 R_n = effective radius of rocket nozzle, ft
 R_s = radius of the LEM heat shield, ft
 t = time elapsed from beginning of LEM descent, sec
 T_0 = surface temperature at initiation of lunation, $^{\circ}K$
 T_d = temperature at bottom of deepest layer, $^{\circ}K$
 T_g = effective exhaust gas temperature, $^{\circ}K$
 T_m = lunar surface temperature, $^{\circ}K$
 T'_m = gradient at the surface, $^{\circ}K\ cm^{-1}$
 T_n = effective exhaust nozzle temperature, $^{\circ}K$
 T_{no} = effective exhaust nozzle temperature before engine cutoff, $^{\circ}K$
 T_s = temperature of the subsolar point, $^{\circ}K$
 $T(x)$ = temperature at depth, x , $^{\circ}K$
 $U's$ = equivalent potential, V

W = radiant emittance of the surface, $W \text{ cm}^{-1}$
 x = distance measured along the propagation of the heat wave, ft
 z = zenith distance of the sun, deg
 β = reciprocal of the thermal wavelength, cm^{-1}
 ϵ_n = radiant emittance of nozzle
 ϵ_m = radiant emittance of lunar surface
 κ = thermal conductivity of lunar surface material, $\text{cal sec}^{-1} \text{ cm}^{-1} \text{ } ^\circ\text{K}^{-1}$
 ρ = density of lunar surface material, gm cm^{-3}
 σ = Stefan-Boltzmann constant, 5.6686×10^{-12} , $W \text{ cm}^{-2} \text{ } ^\circ\text{K}^{-4}$
 τ = minimum time constant of the equivalent circuit, sec
 τ_1 = time constant of the temperature decay of the nozzle after landing, sec

I. INTRODUCTION

An integral part of the Apollo Program is the Lunar Excursion Module known as LEM. The Apollo spacecraft consists of the LEM and adapter, the Service Module, the Command Module, a Boost Cover, and a Launch Escape System. Powered by a three-stage Saturn V launch vehicle, the craft will orbit the Moon. The manned lunar mission will then employ a technique known as Lunar-Orbit rendezvous. This technique will allow the LEM to separate from the Lunar Orbiting Apollo and Service Module.

The function of LEM will be to carry the astronauts during their descent to the lunar surface for exploration. Following this exploration, LEM will return the astronauts to lunar orbit for rendezvous and docking with the Apollo Command and Service Module. Once the docking is accomplished, the spacecraft will then carry out the necessary maneuvers for its return to earth.

Among the important problems facing the LEM is the question of the increased temperature of the landing site during descent, and the cooling rate of the surface after landing. The solution to these questions is vital in the planning and execution of the Apollo mission.

II. SCIENTIFIC OBJECTIVE

The analysis presented in this report aims to determine:

1. The lunar surface temperature brightness at the landing site, as a function of time during and after the descent of the LEM.
2. The variations of temperature brightness at the landing site at specified depths below the surface, as a function of time during and after the descent of the LEM.

The computations have been carried out for models of the lunar surface composed of the following:

1. Homogeneous particulate material.
2. Homogeneous vesicular material.
3. Homogeneous solid material.
4. Particulate surface layer with a substrate of vesicular material.
5. Particulate surface layer with a substrate of solid material.
6. Vesicular surface with a substrate of solid material.
7. Particulate surface with a rubble substrate.
8. Homogeneous rubble.

The output data from the computer program are presented in the following form:

1. Temperature brightness at the surface and to depths down to five subsurface levels at the beginning of the LEM descent.

2. Temperature brightness at the surface and to depths down to five subsurface levels during the LEM descent.
3. Temperature brightness at the surface and to depths down to five subsurface levels after the LEM descent, until the temperature change at each level has been reduced to five per cent of the maximum temperature change induced by the LEM descent.

III. HEAT TRANSFER ON THE LUNAR SURFACE

A. Irradiance on the Surface Produced by LEM

The irradiance Q_{LEM} on the lunar surface produced by the LEM exhaust is given by the following equation:

$$Q_{LEM} = g_c(H,d) (T_g - T_m) + \sigma F_{ns} \epsilon_n T_n^4, \quad (1)$$

where $g_c(H,d)$ is the convection heat-transfer coefficient given in Table I, T_g is the effective exhaust gas temperature, T_m is the lunar surface temperature, σ is the Stefan-Boltzmann constant, ϵ_n is the radiant emittance of the nozzle, T_n is the effective temperature of the exhaust nozzle, and F_{ns} is the view factor from the differential surface element to rocket nozzle.

Eq. (1) is valid for 27.5866 sec after the initiation of LEM descent. Thereafter, $Q_{LEM} = 0$.

The values of F_{ns} are obtained from the following equation:

$$F_{ns} = \frac{1}{2} \left\{ 1 - \frac{(d - R_n)(d + R_n) + H^2}{\sqrt{[(d + R_n)^2 + H^2][(d - R_n)^2 + H^2]}} \right\}, \quad (2)$$

where H , the elevation of LEM above the surface, in feet, is given as a tabulated function of time, d is the distance in feet from LEM point of touchdown and R_n is the effective radius of the rocket nozzle in feet.

For the computation we have taken the following values:

$$\begin{aligned} T_g &= 2493^\circ\text{K} \\ T_n &= 1611^\circ\text{K} \\ \sigma &= 5.6686 \times 10^{-12} \text{ W cm}^{-2} \cdot \text{K}^{-4} \\ \epsilon_n &= 0.90 \\ R_n &= 2.386 \text{ ft} \end{aligned}$$

TABLE I

ELEVATION OF THE LEM ABOVE THE TOUCHDOWN
POINT AND GAS HEAT-TRANSFER COEFFICIENTS AS A FUNCTION OF TIME

Time (t) sec	Height (H) ft	Gas Heat-Transfer Coefficients $g_c(d)$ and $g_c(t)$. $W\text{ cm}^{-2}\text{ }^\circ\text{K}^{-1}$											
		d=0ft	exp	d=5ft	exp	d=10ft	exp	d=20ft	exp	d=50ft	exp	d=100ft	exp
0.0	71.6	1.272	-4	1.277	-4	1.194	-4	0.908	-4	1.977	-5	6.92	-7
1.1	68.7	1.317	-4	1.321	-4	1.231	-4	0.931	-4	1.872	-5	5.70	-7
2.2	66.0	1.397	-4	1.397	-4	1.293	-4	0.963	-4	1.729	-5	4.59	-7
3.3	63.2	1.485	-4	1.482	-4	1.364	-4	0.991	-4	1.519	-5	3.51	-7
4.4	60.5	1.583	-4	1.576	-4	1.439	-4	1.016	-4	1.422	-5	2.68	-7
5.5	57.6	1.701	-4	1.688	-4	1.527	-4	1.042	-4	1.249	-5	1.94	-7
6.6	54.4	1.848	-4	1.825	-4	1.633	-4	1.068	-4	1.058	-5	1.33	-7
7.7	51.2	2.017	-4	1.982	-4	1.749	-4	1.089	-4	0.893	-5	8.76	-8
8.8	48.0	2.214	-4	2.162	-4	1.877	-4	1.101	-4	0.694	-5	5.51	-8
9.9	44.8	2.446	-4	2.372	-4	2.018	-4	1.102	-4	5.288	-6	3.30	-8
11.0	40.9	2.793	-4	2.677	-4	2.207	-4	1.084	-4	3.540	-6	1.63	-8
12.1	36.9	3.244	-4	3.061	-4	2.419	-4	1.033	-4	2.139	-6	7.15	-9
13.2	33.0	3.823	-4	3.534	-4	2.643	-4	0.939	-4	1.138	-6	2.76	-9
14.3	29.0	4.606	-4	4.132	-4	2.851	-4	0.793	-4	0.514	-6	9.07	-10
15.3940	25.8	5.462	-4	4.736	-4	2.982	-4	0.637	-4	2.298	-7	3.74	-10
16.3994	24.0	6.052	-4	5.119	-4	3.019	-4	0.538	-4	1.356	-7	1.59	-10
17.4528	22.1	6.800	-4	5.565	-4	3.016	-4	4.300	-5	7.274	-8	0.74	-10
18.5090	20.2	7.724	-4	6.062	-4	2.953	-4	3.224	-5	3.58	-8	0.28	-10
19.5284	18.3	8.843	-4	6.579	-4	2.813	-4	2.263	-5	1.645	-8	0.11	-10
20.5300	16.2	1.054	-3	7.209	-4	2.526	-4	1.326	-5	5.81	-9	0.05	-10
21.5329	13.8	1.328	-3	7.871	-4	2.006	-4	5.787	-6	1.41	-9	-	-
22.5430	11.4	1.753	-3	8.210	-4	1.302	-4	1.772	-6	2.44	-10	-	-
23.5616	9.0	2.479	-3	7.601	-4	5.744	-5	3.136	-7	0.23	-10	-	-
24.5628	6.5	3.879	-3	5.134	-4	1.223	-5	2.434	-8	-	-	-	-
25.5666	4.7	5.319	-3	1.707	-4	1.043	-6	9.42	-10	-	-	-	-
26.5766	3.1	6.297	-3	1.819	-5	2.851	-8	0.10	-10	-	-	-	-
27.5866	1.6	8.491	-3	8.017	-8	0.28	-10	-	-	-	-	-	-

B. Radiant Emittance From Lunar Surface to Space

The radiant emittance Q_{rs} from the area of the lunar surface affected by the LEM descent is expressed by the equation

$$Q_{rs} = \sigma \epsilon_m (1 - F_{ss}) T_m^4, \quad (3)$$

where T_m is the lunar surface temperature in °K, ϵ_m is the radiant emittance of the lunar surface, F_{ss} is a view factor that takes into account that the surface "sees" part of the shield surrounding the LEM exhaust; the other terms are as defined for Eq. (1).

The term F_{ss} is given by the following expression:

$$F_{ss} = \frac{1}{2} \left\{ 1 - \frac{(d-R_s)(d+R_s) + (H+2.450)^2}{\sqrt{[(d+R_s)^2 + (H+2.450)^2][(d-R_s)^2 + (H+2.450)^2]}} \right\}, \quad (4)$$

where R_s is the radius of the heat shield in feet. Equation (4) is valid for all times. For the computation we take $R_s = 6.750$ feet and 0, 5, 10, 20, 50 and 100 feet for the values of d .

C. Irradiance on the Surface by the Sun

If we take z as the zenith distance of the sun and assume a smooth surface, the irradiance J on a given point on the lunar surface is given by

$$J = J_0 \cos z, \quad (5)$$

where

$$J_0 = \sigma \epsilon_m T_s^4, \quad (6)$$

and

T_s = theoretical temperature of the subsolar point,
°K (assuming no heat conducted inward).

For the purpose of computation the following values are used:

$$\epsilon_m = 0.93$$

and

$$T_s = 395^\circ\text{K}.$$

Moreover, the radiant emittance W of the surface, which is assumed smooth, obeys the Lambert Law and is given by

$$W = \sigma \epsilon_m T_m^4. \quad (7)$$

Calculation of post-descent heat flux produced some problems during checkout. As initially specified, T_g went to 0 at LEM cutoff, but it was also required to retain the attenuation of radiative cooling occurring because the LEM's heat shield cut out part of the sky. These assumptions were finally found to account for an elusive "bug", whose effects were particularly striking at ground zero. The first and most obvious impossibility was that, with part of the sky "missing", calculations gave an equilibrium temperature after cooling that was much higher than the surface temperature prior to the LEM descent. According to Eq. (3), the equilibrium surface temperature would rise up to 150° or 200°K.

Clearly the analysis of heat exchange between LEM and surface after descent was deficient. A proper analysis should more carefully take into account the cooling of the nozzle, the heat exchanged with the heat shield (since the heat shield is radiating and the LEM is still a heat source), and the solar flux (the point

under consideration on the surface could be shaded by the LEM). Unfortunately, schedules did not allow the time for the requisite analysis.

In order to get reasonable results, i.e., correct equilibrium temperatures, during the post descent phase, and due to the exigencies of time and programming difficulties, the input solar flux was attenuated by the same $(1 - F_{ss})$ term as the radiant emittance of the surface. The use of this term, although dubious, may be justified, to some extent, by viewing it as an "average" over shaded and unshaded points in the vicinity of the point under consideration, and because it gives answers that are more reasonable than without it.

The second problem was due to numerical artifacts caused by the sudden "cooling" of the nozzle. In order to smooth them out, an exponential decay of nozzle temperature T_n after LEM cutoff was added. Thus, measuring time, t , from LEM engine cutoff, we have

$$T_n = T_{no} e^{-t/\tau_1}, \quad (8)$$

where τ_1 is the time constant.

IV. ASSUMED THERMAL PARAMETERS FOR THE LUNAR SURFACE

The thermal parameters required in our analysis are thermal conductivity κ , density ρ and specific heat c .

Table II gives these parameters for the assumed materials of the different models.

TABLE II

THERMAL PARAMETERS

Material	Density (ρ)	Specific Heat (c)	Thermal Conductivity (κ)
	g cm^{-3}	$\text{J g}^{-1}\text{K}^{-1}$	$\text{W cm}^{-1}\text{K}^{-1}$
Powder	1.1	$0.502 + 7.4 \times 10^{-4}T$	$4.62 \times 10^{-6} + 3.05 \times 10^{-13}T^3$
Vesicular Rock	0.9	$0.502 + 7.4 \times 10^{-4}T$	$1.50 \times 10^{-3} + 0.2 \times 10^{-5}T$
Rock	2.6	$0.502 + 7.4 \times 10^{-4}T$	$0.02 + 1.0 \times 10^{-5}T$
Rubble	1.9	$0.502 + 7.4 \times 10^{-4}T$	$2.0 \times 10^{-3} + 20 \times 10^{-6}T$

V. LANDING SITE AND TIME

The LEM will land at a point $\pm 5^\circ$ of a given latitude. From the law of variation of lunar temperature and accuracy of the assumptions it will suffice to assume that the LEM will land on the equator. The exact longitude is not yet determined, but the landing site is specified to be at a longitude of 45° with respect to the terminator.

VI. HEAT FLOW EQUATIONS

The heat flow equation in one dimension is simply a statement of the law of conservation of energy, i.e., during a time dt the net heat flux into a slice of material of thickness dx must be manifest as a rise in temperature of the substance. A typical approach is to write this condition, pass to the limit as dx and dt approach 0, and obtain a partial differential equation such as

$$\rho c \frac{\partial T}{\partial t} = \frac{\partial}{\partial x} \left(\kappa \frac{\partial T}{\partial x} \right) + Q(x,t) \quad (9)$$

where ρ = density,
 c = specific heat,
 T = temperature,
 t = time,
 x = depth beneath the lunar surface,
 κ = thermal conductivity,
 $Q(x,t)$ = flux density at depth, x , and time, t .

For numerical computations it is then necessary to undo the limiting process and approximate the partial differential equation with a difference equation. Usually this process tends to mask the physical significance of the difference equation. In fact, it is possible to write the conservation laws directly for the given slices of material, and thus "lump" parameters. The resulting equations turn out to be identical to those obtained by the difference equation technique, but they also retain physical significance so that the physical interpretation of the numerical approximation is clear. See, for example, Volynskii and Bukhman (1) or Saul'yev (2).

As a further advantage the significance and method of treating discontinuities becomes clear. It is useful to consider the electrical analogy of the heat flow equation given in Figure 1. A slice of thickness Δx is represented by the R-C network where

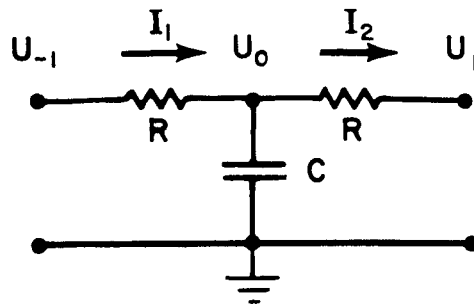


FIG. 1. Electrical Analogy for the heat flow equation and for a thin homogeneous layer.

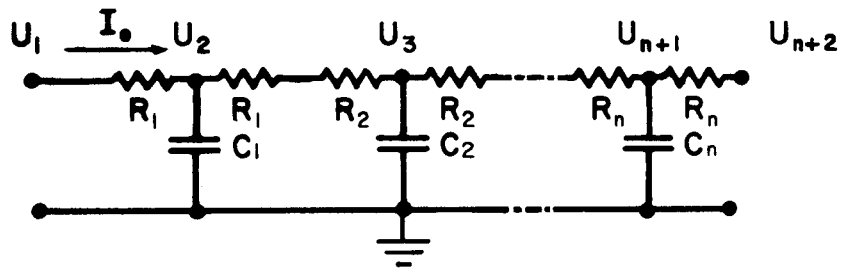


FIG. 2. Electrical analogy for the heat flow equation and for a series of thin homogeneous layers.

$$R = \Delta x / 2\kappa \quad (10)$$

$$C = \rho c \Delta x \quad (11)$$

In this analogy the potential U_0 is proportional to the temperature at the center of the slice, U_{-1} and U_{+1} are proportional to the temperatures at the ends of the slice. I_1 is proportional to the flux into the slice, and I_2 is proportional to flux out, so that $I_1 - I_2$ is proportional to the rate of change of U_0 . For n slices, the analogy is given in Figure 2, where I_0 is equivalent to the input flux at the surface. If we neglect feedback, the minimum time constant of the equivalent circuit is given by

$$\tau = \min_{i=1,n} \{R_i C_i\} \quad (12)$$

as is obvious from inspection of the circuit diagram. Also, it can readily be seen that if the lower boundary constraint is given by

$$\frac{\partial T}{\partial x} = \text{constant} \quad (13)$$

the system is unstable. The constraining $U_{n+2} = \text{const}$, however, yields a stable system.

Figure 2 yields a set of ordinary differential equations. Inspection shows that these may be solved by any of a number of techniques. The simplest and most convenient for the problem at hand is Euler's method, or the method of forward differences, which gives a stable system if the integration step size is taken shorter than τ . This yields a technique for automatic step-size control.

Since the lumped parameters analog system given in Figure 2 yield the same equations as do second central differences, it is easy to see the assumptions implicit in the numerical integration technique. The density, specific heat, and conductivity are assumed constant over one time step. The values are calculated from the depth of the slice, and the temperature at the center of the slice at the beginning of the time step. Furthermore, the input flux is held constant over an integration step.

VII. THERMAL MODELS OF THE LUNAR SURFACE

The following model was used to determine the thermal parameters of the lunar material as a function of temperature T:

$$c = c_0 + c_1 T , \quad (14)$$

$$\kappa = \kappa_0 + \kappa_1 T + \kappa_2 T^3 , \quad (15)$$

where c_0 , c_1 , κ_0 , κ_1 , κ_2 , as well as ρ were presumed to be piece-wise constant functions of depth x . For the purposes of the program and this report, we called the regions of constant c 's and κ 's "layers", as opposed to the "slices" associated with the lumping of parameters. In fact, the number of "slices" to be associated with each "layer" is an input parameter for each layer. The set of six numbers c_0 , c_1 , κ_0 , κ_1 , κ_2 , and ρ is called a "model". Provisions are made for storing up to 20 models in the program. The exact set of parameters to use is then specified on input as a function of the layer number. Provision is made for up to 20 layers, and up to 100 slices.

VIII. INITIAL CONDITIONS

It seemed desirable that the program should be able to allow the input thermal distribution to relax over a lunar day or so, to reduce sensitivity to errors in the initial temperature distribution. The first plan was simply to input a temperature profile and allow it to relax over a time period specified in the input data. During checkout, it became obvious that:

1. The transient response was substantially unaffected by the variations in initial conditions, so long as they were consistent with the thermal model of the moon.
2. The "steady-state" thermal distribution varies rather substantially with the model of lunar composition.

In order to provide a set of consistent initial conditions for the LEM descent which represented the model under consideration, and to avoid hand computations or reliance on external sources for input, the following scheme was adopted.

For a homogeneous medium, with constant coefficients, the thermal distribution at a particular point in time due to a sinusoidal input of angular frequency, ω , can be written in the form

$$T(x) = e^{-\beta x}(A \cos \beta x + B \sin \beta x) + D, \quad (16)$$

where A, B, and D are appropriate constants and

$$\beta = \sqrt{(\rho c \omega / \kappa)} \quad (17)$$

is the reciprocal of the thermal wavelength.

To create approximate initial conditions, we chose as appropriate the time immediately before lunar sunrise. As input parameters, the program accepts surface temperature, T_m , and the temperature, T_d , at the maximum depth under consideration; x , ρ , c , and κ are then calculated on the assumption of a linear temperature distribution:

$$T(x) = T_m + \frac{x}{x_d} (T_d - T_m) . \quad (18)$$

From this, an approximate phase angle

$$P(x) = \int_0^x \sqrt{\rho c \omega / \kappa} dx \quad (19)$$

is calculated. $T(x)$ is then calculated from the formula

$$T(x) = e^{-P(x)} [A \cos P(x) + B \sin P(x)] + D , \quad (20)$$

where A , B , D are chosen so that

$$T(0) = T_m , \quad T(x_d) = T_d ,$$

and the gradient at the surface, T'_m , is consistent with the net flux at the surface. This yields a wave-type set of initial conditions which is roughly consistent with the thermal parameters of the model. This distribution is then relaxed over at least one lunar day before it is used as a set of initial conditions for the LEM descent. In this manner, the program automatically generates a reasonable set of initial conditions, simplifying program usage.

At this point a further problem crops up. Because of the "high frequency" of the input during LEM descent, much thinner slices are needed than during the lunation. Furthermore,

the depth of material which must be considered is substantially less. In order to take account of this, a set of "thick" slices is input for use during lutation and a "thin" set of slices is used during and after the descent phase. Accordingly it is necessary to interpolate the temperature profile obtained from the lutation to the finer mesh required for the descent phase. As became apparent during checkout of the program, this must be done with some care to insure that no artificial transient behavior is induced by interpolating across discontinuities.

At a boundary separating regions of high and of low conductivity, simple linear interpolation will produce the same thermal gradient on both sides of the boundary. Thus, on the side with low conductivity the gradient will be steeper than justified by the flux across the boundary. On the side with high conductivity, the gradient will not be steep enough. This, of course, initiates a wave which will propagate in both directions from the discontinuity. This behavior tends to confuse the results, but is easily avoided by care in treatment of the discontinuity.

IX. BOUNDARY CONDITIONS

Three types of boundary problems exist: at the surface, at the interface between layers in the model, and at the lower level of the region of interest. As has already been remarked, the use of a constant temperature at the lower boundary is most satisfactory from a technical point of view, and offers no programming difficulty. At the boundaries between layers, the discontinuity in $\partial^2 T / \partial x^2$ offers no difficulty since the lumped parameter method makes no assumptions of continuity. The difficulties in the use of the difference equation stem from the limiting process used in defining $\partial^2 T / \partial x^2$; they are not inherent in the physics of the situation. Since the lumped parameter approach avoids limits, it avoids the problem. Consequently, there are no programming difficulties at these boundaries.

At the surface, the condition is substantially different. From Figure 2 it is apparent that the system of differential equations does not determine the surface temperature directly, but only the temperature at the midpoint of the topmost slice. In the numerical integration method used, the input flux is assumed constant over the integration step. How then should the surface temperature be updated? The first approach is simply to note that

$$U_0 - U_1 = I_0 R ,$$

and then update U_0 in such a manner that it follows U_1 precisely. During the course of checkout, a series of bad runs cast doubt on the validity of this procedure. As it turned out, the basic trouble was elsewhere, but in the interim this problem came under scrutiny. Obviously, if U_0 changes over an integration step, the flux radiated by the surface and the convective flux from the LEM also change, thus changing the net input flux. If the surface temperature is simply updated as described above, the updated gradient will not be compatible with the updated flux. In fact,

the gradient will "lag" one integration step behind the flux. Since it appeared that this situation might be causing some of the observed instability, this procedure was abandoned in favor of an iterative procedure to solve for an updated U_0 which would yield a compatible gradient and flux.

After the program was running, the iterative procedure in turn came into question. Obviously with this technique, the surface temperature responds instantaneously to any sharp change in flux, such as, for example, LEM ignition, and LEM cutoff. This response was felt to be physically unjustifiable, yet a study of possible alternatives provided no easy solution. The problem lies in both the physics and the mathematics of the situation. In the first place, absorption and radiation do not take place precisely at the surface: there is some penetration of the surface by incident radiation and some radiation from beneath the surface. At any depth, the partial derivative of absorbed energy with respect to depth, for example, must be finite. This would be an acceptable model to program, given the necessary data and time. On the other hand, in order to adequately simulate the response of the system to a high frequency input (the frequency response of the simulated system is proportional to the square of the slice thickness), we must choose slices thin enough so that the time constant of the system is substantially shorter than the shortest period (highest frequency) in the input signal. Given a step function input, we face difficulties, since a step function has energy at every frequency. Thus it is basically impossible, without using very sophisticated techniques, to simulate the correct response to a step function. After these considerations it was decided to let well enough alone.

X. COMPUTER OUTPUT

We ran the computer program for the proposed eight models. Data from the computer output are presented in Tables III, IV, V, VI, VII, VIII, IX and X.

Figure 3 gives the homogeneous vesicular material temperatures at different depths and as a function of time elapsed from the beginning of the descent of the LEM.

The Tables and the notes at the bottom are self-explanatory.

TABLE III

MAXIMUM TEMPERATURES (°K) AT SURFACE AND SUBSURFACE LOCATIONS
MODEL 1. HOMOGENEOUS PARTICULATE MATERIAL

Dist. from pt. of touchdown, d, (ft)	0	5	10	20	50	100	Pre-descent Temperatures
Depth (cm)							
0	1640 (28)	811 (22)	600 (21)	476 (13)	383 (5)	363 (5)	361
0.1	807 (46)	425 (90)	380 (90)	365 (100)	358 (110)	356**	356
0.2	539 (170)	375 (350)	358 (350)	354 (350)	352 (400)	352**	352
0.5	383 (1800)	342*	338*	337*	337*	336**	336
1.0	313*	311**	311**	311**	311**	311**	310
2.0	262**	262**	262**	262**	262**	262**	261

Notes:

At depths greater than those indicated, the temperature approaches 230°K

Values in parentheses are times (in seconds after initiation of descent) at which maximum temperature occurs

*Temperature rising at end of calculations (2000 sec)

**Temperature within one degree of pre-descent temperature at 2000 sec

TABLE IV
MAXIMUM TEMPERATURES (°K) AT SURFACE AND SUBSURFACE LOCATIONS
MODEL 2. HOMOGENEOUS VESICULAR MATERIAL

Dist. from pt. of touchdown, d, (ft)	0	5	10	20	50	100	Predescent Temperatures
Depth (cm)							
0	1490 (28)	573 (26)	441 (22)	383 (15)	356 (8)	353** (8)	352
0.2	718 (34)	446 (30)	394 (27)	367 (23)	353 (20)	352** (18)	351
0.5	527 (60)	394 (60)	369 (50)	357 (44)	351** (44)	351**	350
1.0	437 (160)	369 (150)	357 (130)	351 (130)	348** (130)	348**	348
2.0	386 (550)	353 (500)	347 (450)	345 (450)	344**	344**	344
5.0	346*	334*	332**	332**	332**	332**	331

Notes:

At depths greater than those indicated, the temperature approaches 230°K

Values in parentheses are times (in seconds after initiation of descent) at which maximum temperature occurs

*Temperature rising at end of calculations (2000 sec)

**Temperature within one degree of predescent temperatures at 2000 sec or at maximum temperature

TABLE V

MAXIMUM TEMPERATURES (°K) AT SURFACE AND SUBSURFACE LOCATIONS
MODEL 3. HOMOGENEOUS SOLID MATERIAL

Dist. from pt. of touchdown, d, (ft)	0	5	10	20	50	100	Predescent Temperature
Depth (cm)							
0	705 (28)	365 (26)	334 (22)	321 (15)	315** (8)	315** (7)	315
0.4	405 (36)	334 (32)	323 (27)	317 (23)	314** (21)	314** (19)	314
1.0	354 (70)	322 (60)	317 (60)	314 (48)	313** (48)	314**	313
2.0	332 (180)	316 (160)	313 (170)	312**	312**	312**	311
6.0	311 (1100)	306** (800)	306**	306**	306**	306**	305
10.0	302*	300** (1800)	300**	300**	300**	300**	299

Notes:

Values in parentheses are times (in seconds after initiation of descent) at which maximum temperature occurs

*Temperature rising at end of calculations (2000 sec)

**Temperature within one degree of predescent temperature at 2000 sec or at maximum temperature

TABLE VI

MAXIMUM TEMPERATURES (°K) AT SURFACE AND SUBSURFACE LOCATIONS
 MODEL 4. PARTICULATE SURFACE LAYER WITH SUBSTRATE OF VESICULAR MATERIAL

(Particulate Layer 0.1 cm thick)

Dist. from pt. of touchdown, d, (ft)	0	5	10	20	50	100	Predescent Temperatures
Depth (cm)							
0	1640 (28)	775 (28)	600 (21)	472 (13)	377 (5)	357 (3)	355
0.1	607 (38)	348 (60)	323 (70)	316 (70)	312** (80)	312**	311
0.2	433 (60)	320 (120)	312 (120)	310 (130)	309**	309**	308
0.5	381 (110)	316 (180)	310 (180)	308** (200)	308**	308**	307
1.0	348 (250)	311 (300)	307** (300)	306**	306**	306**	306
6.0	295*	291**	291**	291**	290**	290**	290

Notes:

At depths greater than those indicated, the temperature approaches 230°K

Values in parentheses are times (in seconds after initiation of descent) at which maximum temperature occurs

*Temperature rising at end of calculations (2000 sec)

**Temperature within one degree of predescent temperature at 2000 sec or at maximum temperature

TABLE VII

MAXIMUM TEMPERATURES (°K) AT SURFACE AND SUBSURFACE LOCATIONS
 MODEL 5. PARTICULATE SURFACE LAYER WITH SUBSTRATE OF SOLID MATERIAL

(Particulate Layer 0.1 cm thick)

Dist. from pt. of touchdown, d, (ft)	0	5	10	20	50	100	Predescent Temperature
Depth (cm)							
0	1639 (28)	773 (28)	597 (21)	468 (13)	370 (5)	350**	349
0.1	531 (38)	294 (60)	269 (70)	262 (80)	259*	259*	257
0.3	275 (60)	253 (130)	251** (150)	251** (170)	251**	251**	250
0.5	270 (80)	252 (150)	251** (160)	251** (180)	251**	251**	250
1.1	263 (130)	251** (200)	250** (250)	250**	250**	250**	250
2.1	257 (300)	250** (350)	250** (450)	250**	250**	250**	250

Notes:

At depths greater than those indicated, the temperature approaches 230°K

Values in parentheses are times (in seconds after initiation of descent) at which maximum temperature occurs

*Temperature rising at end of calculations (2000 sec)

**Temperature within one degree of predescent temperature at 2000 sec or at maximum temperature

TABLE VIII

MAXIMUM TEMPERATURES (°K) AT SURFACE AND SUBSURFACE LOCATIONS
MODEL 6. VESICULAR MATERIAL SURFACE LAYER WITH SUBSTRATE OF SOLID MATERIAL

(Vesicular Layer 1.25 cm thick)

Dist. from pt. of touchdown, d, (ft)	0	5	10	20	50	100	Pre-descent Temperatures
Depth (cm)							
0	1435 (28)	549 (26)	414 (22)	354 (15)	326 (7)	323** (7)	322
0.1	874 (32)	465 (27)	384 (25)	343 (20)	323 (13)	321** (13)	321
0.5	500 (60)	361 (60)	335 (50)	322 (45)	315** (45)	315**	314
1.25	333 (170)	310 (150)	306 (150)	304** (150)	304**	304**	303
4.0	308 (700)	300** (550)	300** (800)	299**	299**	299**	299
8.0	297 (1700)	294** (1300)	294**	294**	294**	294**	293

Notes:

At depths greater than those indicated, the temperature approaches 230°K

Values in parentheses are times (in seconds after initiation of descent) at which maximum temperature occurs

*Temperature rising at end of calculations (2000 sec)

**Temperature within one degree of pre-descent temperature at 2000 sec or at maximum temperature

TABLE IX

MAXIMUM TEMPERATURES (°K) AT SURFACE AND SUBSURFACE LOCATIONS
MODEL 7. PARTICULATE SURFACE LAYER WITH SUBSTRATE OF RUBBLE

(Particulate Layer 0.1 cm thick)

Dist. from pt. of touchdown, d, (ft)	0	5	10	20	50	100	Pre-descent Temperatures
Depth (cm)							
0	1640 (28)	809 (25)	599 (21)	471 (13)	375 (5)	354** (3)	353
0.1	578 (38)	330 (60)	306 (70)	299 (70)	296** (100)	296**	295
0.2	367 (60)	298 (130)	293 (130)	292** (150)	291**	291**	291
0.5	331 (140)	295 (200)	291** (200)	290** (250)	290**	290**	290
1.0	310 (350)	291 (400)	289** (450)	289**	289**	289**	288
6.0	274**	273**	273**	273**	273**	273**	273

Notes:

At depths greater than those indicated, the temperature approaches 230°K

Values in parentheses are times (in seconds after initiation of descent) at which maximum temperature occurs

*Temperature rising at end of calculations (2000 sec)

**Temperature within one degree of pre-descent temperature at 2000 sec or at maximum temperature

TABLE X

MAXIMUM TEMPERATURES (°K) AT SURFACE AND SUBSURFACE LOCATIONS
MODEL 8. HOMOGENEOUS RUBBLE

Dist. from pt. of touchdown, z, (ft)	0	5	10	20	50	100	Predescent Temperatures
Depth (cm)							
0	1370 (28)	506 (26)	407 (22)	367 (14)	349 (7)	347** (6)	346
0.2	556 (38)	397 (32)	368 (27)	354 (25)	346 (21)	345** (20)	345
0.5	438 (90)	366 (80)	353 (70)	347 (70)	344** (60)	344**	344
1.0	388 (250)	352 (250)	345 (200)	343 (250)	341**	341**	341
2.0	358 (900)	340 (750)	338 (850)	337*	336**	336**	336
5.0	326*	322*	321**	321**	321**	321**	320

Notes:

At depths greater than those indicated, the temperature approaches 230°K

Values in parentheses are times (in seconds after initiation of descent) at which maximum temperature occurs

*Temperature rising at end of calculations (2000 sec)

**Temperature within one degree of predescent temperature at 2000 sec or at maximum temperature

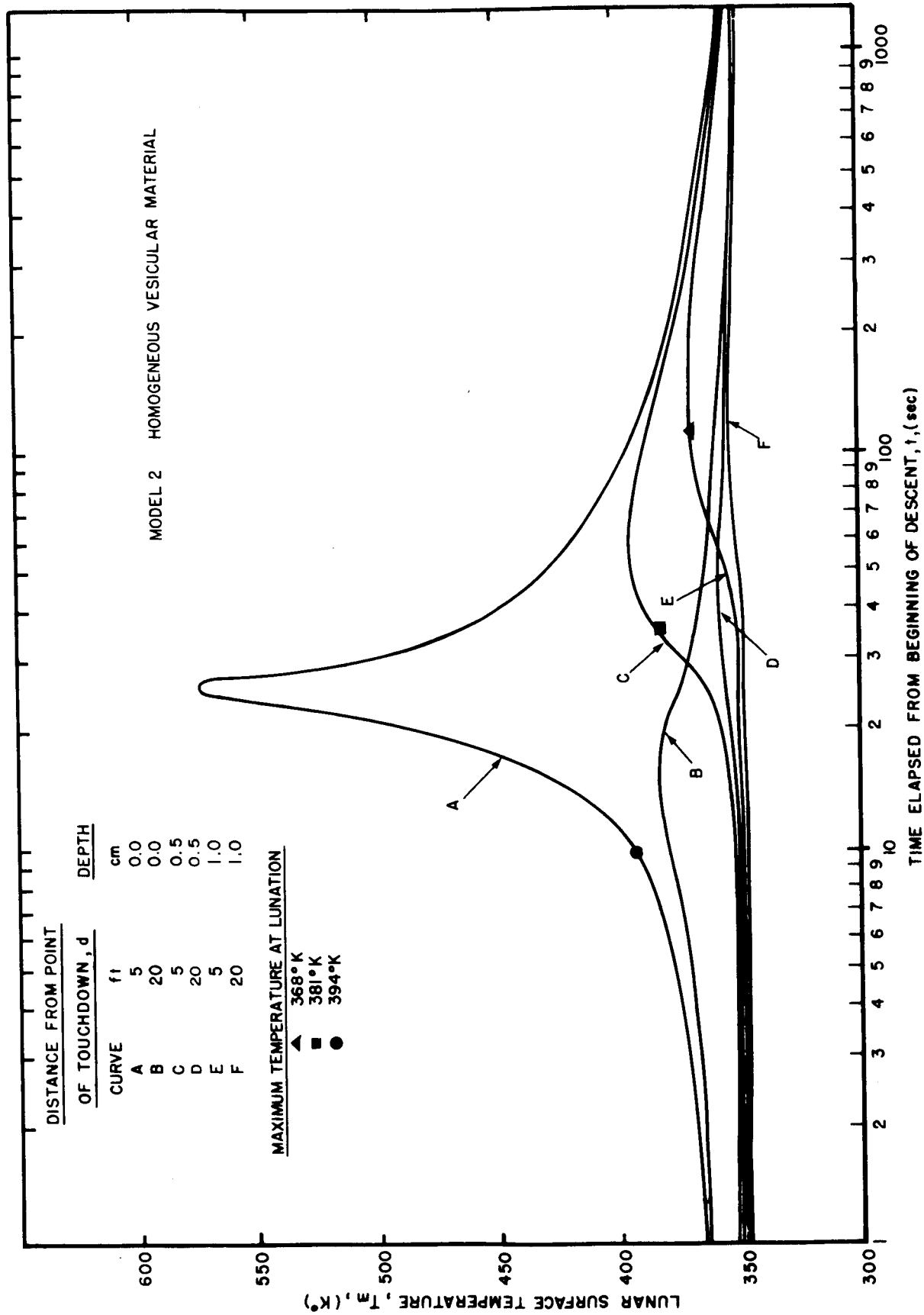


FIG. 3. Variation of surface and subsurface temperature vs. time (plots based on computer output).

APPENDIX A

DISCUSSION OF THE COMPUTER PROGRAM

In the Infrared Group a program has been written* to solve the heat-conduction equation in the lunar surface. At the beginning of the project we planned to modify the existing program but this plan was abandoned. For the following reasons a new program was written: a) the existing program did not have models of conductivity and specific heat sufficiently general, b) the integration step size control seemed inadequate, c) the existing program carried out several complex computations which were not germane to the problem at hand, d) the existing program failed to decouple the lunar thermal model from the heat equation. Thus each thermal model would have to be substituted analytically into the heat equation to make a heat equation for each model. This risky programming procedure requires multiple transcriptions of the basic equations, multiplies the chances of error, increases "debugging" time, and decreases confidence that all bugs have been found.

Since the FORTRAN listings provide a detailed and absolutely unambiguous description of the program, we shall confine the English language discussion to a sketch of the general flow of the program.

The logical structure of the program approximates, so far as is possible, the structure of the problem. The program itself decomposes into several subroutines, each charged with a specific task. Each subroutine represents, in a sense, an abstraction of a particular part of the problem. Subroutine HFSTP, for example, which actually does the integration, simply solves the analog system of Figure 2. Subroutine EVMODL evaluates the coefficients of

*A Computer Program to Solve the Heat-Conduction Equation in the Lunar Surface for Temperature-Dependent Thermal Properties, by Jeffrey L. Linsky, Scientific Report No. 7, NASA Grant NsG 64-60.

the system, paying no attention to their possible uses. Subroutines BMDLEM and SFMODL calculate incident flux on the surface due to the LEM and the Sun respectively, again with no regard to the use of these calculations. Subroutine HETFLO controls the progress of the numerical integration, basically in a manner which depends neither on the particular choice of integration techniques nor on the particular configuration of the system. Subroutine SAMPLE samples the results and prints out selected results without concerning itself with the manner in which those results are generated.

This program uses several features peculiar to FORTRAN IV, Version 13. These include labeled COMMON, NAMELIST, and multiple subroutine entries. Labeled COMMON provides a simple method of making data available to a subroutine in the case where it functions as parametric data rather than as input or output. NAMELIST provides the capability for free-form parameter input. Multiple subroutine entries provide a means for initializing subroutines and for simplifying data logistics. These features of the FORTRAN IV language are discussed in reference (3).

APPENDIX B

SAMPLE DECK MAKE UP

1. \$JOB card. "\$JOB" in columns 1-4, account number and name starting in column 16.
2. \$EXECUTE IBJOB card. "\$EXECUTE" beginning in column 1, "IBJOB" beginning in column 16.
3. \$IBJOB card. "\$IBJOB" in column 1, "FIOCS" in column 16.
4. Program decks, in any order. These must include MAIN, QMODLD, MISCD, SBTND, NTRPLT, EVMDLD, SAMPLD, SFMDLD, HETFLD, CREDEP, and HFSTPD.
5. End-file card. 7-8 punch in column 1.
6. Data for NAMELIST DATA. "\$DATA", followed by at least one blank, beginning in column 2.

The variables which must be entered are:

XI, ETA: lunar coordinates of the point to be studied.
SLONG: initial longitude of the sub-solar point.
ESST: theoretical subsolar point temperature.
EB: radiant emissivity.
SB: Stefan-Boltzmann constant.
EMOON: emissivity of the moon.
TNOZ: temperature of LEM nozzle (in degrees Kelvin).
TGAS: temperature of LEM exhaust (in degrees Kelvin).
DIST: table of distances from ground zero for which LEM data is to be input.
NDIST: number of distances for which descent is to be studied (≤ 6).
NLMDP: number of data points in LEM descent profile.
MODELS: number of models of lunar material to be input.

7. Table of times in LEM descent. Exactly NLMDP points must be entered in a 6E12.8 format.
8. Table of LEM altitudes. Exactly NLMDP points must be entered in a 6E12.8 format.
9. Table of gas coefficients. Exactly one card for each of NLMDP points in the trajectory. Each card must contain at least NDIST coefficients in 6E12.8 format.
10. Table of lunar models. Exactly MODELS cards must be present. Each card contains six numbers in 6E12.8 format:
The first card represents MODEL(1), the second MODEL(2), etc.
11. Data for NAMELIST LUNCON. Lunation control parameters. The variables which must be entered are:

LAYERS: the number of layers to be used in the lunar model.

MODEL: a list of model numbers, one per layer.

APPENDIX C
PROGRAM LISTING

```
SIRFTC MAIN LIST,SDD
  INTGFR SLICES,DSLICE
  LOGICAL FIRST,MORE,MOREL
  EXTERNAL QMDLEM,SFMDL
  DIMENSION TSAMPL(50),DSAMPL(50)
  COMMON /TLEM/TLEM(50) /HEIGHT/HEIGHT(50) /GCOEF/GCOEF(50,6)
  C /ARRM1/ LSLICE(20),DEPTH(150),TEMP(150),DEPTHL(102)
  C,TEMPL(102),DEPTHD(102),TEMPZ(102),TEMPD(102),SLICES(20)
  C,DSLICE(20)
  C /DCLV1/MODELS,NDIST,FIRST,MORE,MOREL,NS,TS,DS,LAYERS,NSLICL,%I
  C,ETA,SLONG,SLONGD,ANG,TIMLUN,ALPHA,NSLICD,I
  C /TSSF/ESST /EB/EB /THICK/THICK(20) /TMODL/TMOD(6,20)
  C /SRATE/SRATE
  C /LFMGFO/RADN,RADS,SNS /DIST/DIST(6) /STEBO/SB /EMN/ENOZ
  C /EMN/EMOON /NLEM/NLMDP /TGAS/TGAS /TNOZ/TNOZ /DTR/DTR
  C /MODEL/MODEL(20) /SAMPAR/TSAMPL,DSAMPL,NSAMPL
  C /TAUN/TAUN
  EQUIVALENCE (EMMN,EMOON)
  NAMELIST /DATA/NLMDP,NTDP,NDIST,SLONG,TGAS,TNOZ,DIST,MODELS,XI
  N ,ETA,FSST,ER,SB,EMOON,ENOZ
  N,RADN,RADS,SNS
  N,TAUN
  N/LUNCON/LAYERS,MODEL,SLICES,THICK,TSAMPL,DSAMPL,NSAMPL,SLONGD
  N,ALPHA
  N,MORE
  N,LSLICE
  N,TAUL,LMAX
  N,STEMP,DTEMP
  N /DESCON/SLICES,TSAMPL,DSAMPL,NSAMPL,TIME,NPTMX
  N,DSLICE
  N,MORE
  N,TAUD
  SRATE=360./ .2551443E07
  DTR=3.1415927/180.
  MODELS=3
  NDIST=6
  40 CONTINUE
  READ (5,DATA)
  WRITE (6,DATA)
  READ (5,100) (TLEM(I),I=1,NLMDP)
  WRITE (6,200)
  200 FORMAT(1H010X4HTLEM)
  WRITE (6,800) (TLEM(I),I=1,NLMDP)
  READ (5,100) (HEIGHT(I),I=1,NLMDP)
  WRITE (6,300)
  300 FORMAT(1H010X6HHEIGHT)
  WRITE (6,800) (HEIGHT(I),I=1,NLMDP)
  READ (5,100) ((GCOEF(I,J),J=1,6),I=1,NLMDP)
  WRITE (6,400)
  400 FORMAT(1H010X5HGCOEF)
  WRITE (6,800) ((GCOEF(I,J),J=1,6),I=1,NLMDP)
  READ (5,100) ((TMOD(I,J),I=1,6),J=1,MODELS)
  WRITE (6,500)
  500 FORMAT(1H010X4HTMOD)
  WRITE (6,800) ((TMOD(I,J),I=1,6),J=1,MODELS)
  800 FORMAT(X,1P6F20.8)
  100 FORMAT(6E12.8)
  STEMP=90.
```

```
DTEMP=230.
FIRST=.TRUE.
30 MORE=.FALSE.
  READ (5,LUNCON)
  WRITE (6,LUNCON)
  MOREL=MORE
107 CONTINUE
  CALL CREDEP(LAYERS,LSLICE,THICK,DEPTHL,NSLICL)
117 CONTINUE
  DEPTH(1)=0.
  DEPTH(2)=DEPTHL(NSLICL)
  NTDP=2
  TEMP(1)=STEMP
  TEMP(2)=DTFMP
  CALL NTRPLT(DEPTH,TEMP,NTDP,DEPTHL,TEMP,NSLICL)
127 CONTINUE
  CALL SFMDLI(XI,ETA,SLONG)
137 CONTINUE
  CALL EVMDLI(LAYERS,LSLICE)
147 CONTINUE
  ANG=SLONGD-SLONG
  IF(ANG.LT.0.) ANG=ANG+360.
  TIMLUN=ANG/SRATE
  DIMENSION R(100),C(100)
  NS2=NSLICL-2
  NS1=NSLICL-1
  CALL FVMODL(R,C,TEMP)
  CUR=SFMODL(0,TEMP,FMS)-SB*EMMN*TEMP(1)**4
  OMEGA=DTR*SRATE
  DO 1776 I=1,NS2
1776 C(I)=.5*SQRT(R(I)*C(I)*OMEGA)
  TMP=TEMP(NSLICL)
  DU=TEMP(1)-TMP
  RI=R(I)*CUR
  RI=-RI
  P=C(1)
  DO 1789 I=2,NS1
  TEMP(I)=TMP+EXP(-P)*(DU*(SIN(P)+COS(P))+RI*SIN(P)/C(I-1))
1789 P=P+C(I-2)+C(I-1)
  CALL HETFLO(NSLICL,TEMP,ALPHA,TIMLUN,SFMODL,LMAX,DEPTHL)
157 CONTINUE
  FIRST=.FALSE.
  20 MORE=.FALSE.
  READ (5,DESCON)
  WRITE (6,DESCON)
167 CONTINUE
  CALL CREDEP(LAYERS,DSLICE,THICK,DEPTHD,NSLICD)
  DIMENSION TMPL(102),DPT(102)
  CALL EVMODL(R,C,TEMP)
  TMPL(1)=TEMP(1)
  DO 1848 I=2,NS1
1848 TMPL(I)=(R(I)*TEMP(I)+R(I-1)*TEMP(I+1))/(R(I-1)+R(I))
  DPT(1)=0.
  K=2
  DO 1917 I=1,LAYERS
  LS=LSLICE(I)
  DX=THICK(I)/FLOAT(LS)
  DO 1917 J=1,LS
```

```
DPT(K)=DPT(K-1)+DX
1917 K=K+1
      CALL NTRPLT(DPT,TMPL,NS1,DEPTHD,TEMPZ,NSLICD)
      CALL FVMDLI(LAYERS,DSLICE)
197  CONTINUE
      DO 10 I=1,NDIST
      WRITE (6,201) DIST(I)
201  FORMAT(28H DISTANCE FROM GROUND ZERO = F6.0)
      CALL MOVE(TEMPZ,TEMPD,NSLICD)
207  CONTINUE
      CALL SFMDLI(XI,ETA,SLONGD)
      CALL QMODLI(I)
217  CONTINUE
10   CALL HETFLO(NSLICD,TEMPD,ALPHA,TIME,QMDLEM,NPTMX,DEPTHD)
      IF(MORE) GO TO 20
      IF(MOREL) GO TO 30
      GO TO 40
      END
```

```
$IBFTC QMODLD LIST,SDD
  FUNCTION QMDLEM(TIME,U,FMS)
  DIMENSION U(102)
  COMMON /TLEM/TLEM(50) /STEBO/SB/EMN/EMN/EMMN/EMMN /NLEM/NLEM
  C /VLINK/I,ALPHA,BETA
  C /TGAS/TGAS /TNOZ/TNOZ /GCOEF/GCOEF(50,6) /HEIGHT/HEIGHT(50)
  C /DIST/DIST(6)
  C /LEMGFC/      RADN,RADS,SNS
  C /QVAR1/HV,FNS,FMS,DST,TNOZ4
  C /TAUN/TAUN
  GO TO 50
  ENTRY QMODLI(KDIST)
  TNOZ4=TNOZ**4
  STNOZ4=SB*EMN*TNOZ4
  AP=4./TAUN
  DST=DIST(KDIST)
  I=2
  RETURN
50 CONTINUE
  QMDLEM=SFMODL(TIME,DUM,DUM)
30 IF(TIME.LE.TLEM(I)) GO TO 10
  IF(I.GF.NLEM) GO TO 20
  I=I+1
  GO TO 30
10 CONTINUE
  BETA=(TIME-TLEM(I-1))/(TLEM(I)-TLEM(I-1))
  ALPHA=1.-BETA
  HV=V(HFIGHT)
  FNS=SBTND(DST,RADN,HV)
  FMS=SBTND(DST,RADS,HV+SNS)
  QMDLEM=QMDLEM*(1.-FMS)
  QMDLEM=QMDLEM+(TGAS-U(1))*V(GCOEF(1,KDIST))+FNS*STNOZ4
  GO TO 40
20 FMS=SBTND(DST,RADS,SNS)
  QMDLEM=QMDLEM*(1.-FMS)
  QMDLEM=QMDLEM+FNS*STNOZ4*EXP(AP*(TLEM(I)-TIME))
40 CONTINUE
  RETURN
  END
```

```
SIBETC MISC0  
  FUNCTION V(TABLE)  
  COMMON /VLINK/I,ALPHA,BETA  
  DIMENSION TABLE(1)  
  V=ALPHA*TABLE(I-1)+BETA*TABLE(I)  
  RETURN  
  ENTRY MOVE(A,B,N)  
  DIMENSION A(N),B(N)  
  DO 10 I=1,N  
10 B(I)=A(I)  
  RETURN  
  END
```

```
$IRFTC SBTND  
FUNCTION SBTND(D,R,H)  
DM=D-R  
DP=D+R  
HS=H*H  
SBTND=.5*(1.-(DM*DP+HS)/SQRT((DP*DP+HS)*(DM*DM+HS)))  
RETURN  
END
```

```
*IRFIC NTRPLT
SUBROUTINE NTRPLT(XA,YA,NA,XB,YB,NB)
DIMENSION XA(1),YA(1),XB(1),YB(1)
J=2
DO 10 I=1,NB
40 IF(XB(I).LT.XA(J-1)) GO TO 20
IF(XB(I).LE.XA(J)) GO TO 30
J=J+1
IF(J.LE.NA) GO TO 40
YB(I)=YA(NA)
GO TO 10
20 YB(I)=YA(J-1)
GO TO 10
30 BETA=(XB(I)-XA(J-1))/(XA(J)-XA(J-1))
ALPHA=1.-BETA
YB(I)=ALPHA*YA(J-1)+BETA*YA(J)
10 CONTINUE
RETURN
END
```

```
$IBFTC FVMDLD LIST,SDD
  SURROUTINE FVMODL(R,CA,U)
  COMMON /THICK/DELTA(20) /TMODL/C(6,20) /MODEL/MODEL(20)
  GO TO 30
  ENTRY FVMDLI(NLAYFR,ISLICE)
  DIMENSION ISLICE(20)
  D ,R(100),CA(100),U(102)
  RETURN
30 CONTINUE
  J=1
  DO 20 LAYER=1,NLAYER
  K=ISLICE(LAYER)
  DX=DELTA(LAYER)/FLOAT(K)
  M=MODEL(LAYER)
  RHO=C(1,M)
  DO 20 I=1,K
  SH=C(2,M)+U(J+1)*C(3,M)
  CAPPAC=C(4,M)+U(J+1)*(C(5,M)+C(6,M)*U(J+1)**2)
  R(J)=.5*DX/CAPPAC
  CA(J)=DX*RHO*SH
20 J=J+1
  RETURN
  END
```



```
FIRETC SAMPLE LIST,SDD
SUBROUTINE SAMPLI(DEPTH,U,NPTS,TIME,TIMNXT)
COMMON /SAMPAR/STIME,SDEPTH,ND
DIMENSION SDEPTH(50),STIME(50)
DIMENSION DP(50),TP(50)
DP(1)=0.
ND=1
I=-1
30 I=I+2
IF(I.GT.50 .OR. SDEPTH(I).LT.0.) GO TO 10
20 ND=ND+1
DP(ND)=DP(ND-1)+SDEPTH(I)
IF(ND.EQ.50) GO TO 10
IF(DP(ND).LT.SDEPTH(I+1)-.01*SDEPTH(I)) GO TO 20
GO TO 30
10 CONTINUE
WRITE (6,100) (DP(I),I=1,ND)
TIMNXT=TIME
I=1
ENTRY SAMPLE
IF(TIME.LT.TIMNXT) RETURN
TIMNXT=TIME+STIME(I)
IF(STIME(I+1).LT.0. .OR. I.EQ.49) GO TO 40
IF(TIMNXT.GT.STIME(I+1)-.001*STIME(I)) I=I+2
40 CONTINUE
ENTRY SAMPLC
CALL NTRPLT(DEPTH,U,NPTS,DP,TP,ND)
WRITE (6,200) TIME,(TP(J),J=1,ND)
100 FORMAT(1H0,20X,30HSAMPLE DEPTHS (IN CENTIMETERS)/(X,8F15.4))
200 FORMAT(1H0,10X,6HTIME = E20.8,X,7HSECONDS/(X,8F15.2))
RETURN
END
```

```
$IBFTC SFMDLD LIST,SDD
      FUNCTION SFMODL(TIMF,TEMP,FMS)
      COMMON /DTR/DTR /STEBO/SB /TSSF/TSSF /EB/EB /SRATE/SRATE
      GO TO 107
      ENTRY SFMDLI(XI,ETA,SLI)
      ZETA=SQRT(1.-XI**2-ETA**2)
      SFLUX=SB*EB*ZETA*TSSF**4
      RETURN
107 CONTINUE
      FMS=0.
      IF(TIMF.LT.0.) RETURN
      SLONG=SLI+SRATE*TIME
      SLONG=AMOD(SLONG+180.,360.)-180.
      SFMODL=0.
      IF(SLONG.LE.-90..OR.SLONG.GE.90.) RETURN
      SFMODL=SFLUX*COS(DTR*SLONG)
      RETURN
      END
```

```
SIBFIC HETFLO LIST,SDD
SUBROUTINE HETFLO(NPTS,U,ALPHA,TIMIN,QMDLEM,NSTPMX,DEPTH,KDIST)
COMMON /EMMN/EMMN /STEBO/SB
DIMENSION R(100),C(100)
D,U(102)
107 CONTINUE
ISTEP=0
NSLICE=NPTS-2
TIME=0.
CALL SAMPLI(DEPTH,U,NPTS,TIME,TIMNXT)
CALL HFSTPI(U,R,C,NSLICE,QIN,H)
50 CALL FVMODL(R,C,U)
TAU=R(1)*C(1)
DO 10 I=2,NSLICE
10 TAU=AMIN1(R(I)*C(I),TAU)
QIN=QMDLEM(TIME,U,FMS)
CC=SP*EMMN*U(1)**3
QIN=QIN-CC*U(1)*(1.-FMS)
H=ALPHA*TAU
IF(TIME.LT.TIMIN) H=AMIN1(H,TIMIN-TIME)
H=AMIN1(H,TIMNXT-TIME)
D=U(2)
DD=U(1)
CALL HFSTP
X=DD+1.
DEL=1.
QIN=QIN-(DD-U(2))/R(1)
58 Q=QMDLEM(TIME,X,FMS)
Q=Q-SB*EMMN*(1.-FMS)*X**4-(X-U(2))/R(1)
DEL=-Q*DEL/(Q-QIN)
X=X+DEL
IF(ABS(DEL).LT..1) GO TO 57
QIN=Q
GO TO 58
57 U(1)=X
TIME=TIME+H
CALL SAMPLE
ISTEP=ISTEP+1
IF(TIME.GE.TIMIN) GO TO 60
IF(ISTEP.GE.NSTPMX) GO TO 40
GO TO 50
40 WRITE (6,100) ISTEP
100 FORMAT(1H0,10X,43HHETFLO TERMINATED ON ISTEP CONTROL. ISTEP= 151
60 CALL SAMPLC
RETURN
END
```

```
$IBFTC CRFDEP
SUBROUTINE CREDFP(NLAYER,ISLICE,THICK,DEPTH,NSLICE)
DIMENSION ISLICE(1),THICK(1),DEPTH(1)
J=2
DEPTH(1)=0.
DEPTH(2)=0.
DO 20 I=1,NLAYER
K=ISLICE(I)
DX=THICK(I)/FLOAT(K)
DEPTH(J)=DEPTH(J)+DX/2.
J=J+1
IF(K.EQ.1) GO TO 20
DO 10 L=2,K
DEPTH(J)=DEPTH(J-1)+DX
10 J=J+1
20 DEPTH(J)=DEPTH(J-1)+DX/2.
NSLICE=J
RETURN
END
```

```
$IBFIC HESTPD LIST,SDD
SUBROUTINE HESTPI(U,R,C,N,QIN,H)
DIMENSION U(102),R(100),C(100)
NM1=N-1
107 CONTINUE
RETURN
ENTRY HESTP
DP=((U(3)-U(2))/(R(1)+R(2))+QIN)/C(1)
DO 10 I=2,NM1
CA=1./(R(I-1)+R(I))
CB=1./(R(I)+R(I+1))
D=( U(I)*CA + U(I+2)*CB - U(I+1)*(CA+CB) )/C(I)
U(I)=U(I)+H*DP
10 DP=D
D=((U(N)-U(N+1))/(R(N-1)+R(N))- (U(N+1)-U(N+2))/R(N))/C(N)
U(N)=U(N)+H*DP
U(N+1)=U(N+1)+H*D
U(1)=U(2)+R(1)*QIN
117 CONTINUE
RETURN
END
```

REFERENCES

1. B. A. Volynskii and V. Ye. Bukhman, Analogues for the Solution of Boundary-Value Problems. Translated by Jacques J. Schorr-Kon, translation edited by J. G. L. Michel. Oxford, New York: Pergamon, 1965.
2. V. Saul'yev, Integration of Equations of Parabolic Type by the Method of Nets. Translated (from Russian) by G. J. Tee, translation edited by K. L. Steward. New York: Macmillan Co., 1964.
3. IBM 7090/7094 IBSYS Operating System, Version 13, FORTRAN IV Language, Form C28-6390-2, an unpublished manual by the International Business Machines Company, 1965.